View metadata, citation and similar papers at core.ac.uk

brought to you by CORE

provided by Elsevier - Publisher Connector

Available online at www.sciencedirect.com

ScienceDirect

Nuclear Physics B 796 (2008) 274–293

NUCLEAR PHYSICS B

www.elsevier.com/locate/nuclphysb

Entanglement as a probe of confinement

Igor R. Klebanov [a], David Kutasov [b], Arvind Murugan [a,*]

[a] *Department of Physics and Center for Theoretical Physics, Princeton University, Princeton, NJ 08544, USA*
[b] *Department of Physics, University of Chicago, 5640 S. Ellis Av., Chicago, IL 60637, USA*

Received 5 November 2007; accepted 10 December 2007

Available online 23 December 2007

Abstract

We investigate the entanglement entropy in gravity duals of confining large N_c gauge theories using the proposal of [S. Ryu, T. Takayanagi, Phys. Rev. Lett. 96 (2006) 181602, hep-th/0603001; S. Ryu, T. Takayanagi, JHEP 0608 (2006) 045, hep-th/0605073]. Dividing one of the directions of space into a line segment of length l and its complement, the entanglement entropy between the two subspaces is given by the classical action of the minimal bulk hypersurface which approaches the endpoints of the line segment at the boundary. We find that in confining backgrounds there are generally two such surfaces. One consists of two disconnected components localized at the endpoints of the line segment. The other contains a tube connecting the two components. The disconnected surface dominates the entropy for l above a certain critical value $l_{\rm crit}$ while the connected one dominates below that value. The change of behavior at $l = l_{\rm crit}$ is reminiscent of the finite temperature deconfinement transition: for $l < l_{\rm crit}$ the entropy scales as N_c^2, while for $l > l_{\rm crit}$ as N_c^0. We argue that a similar transition should occur in any field theory with a Hagedorn spectrum of non-interacting bound states. The requirement that the entanglement entropy has a phase transition may be useful in constraining gravity duals of confining theories.
© 2008 Elsevier B.V. All rights reserved.

PACS: 12.38.Aw; 11.15.Pg; 11.25.Tq; 05.70.Fh; 03.67.Mn; 03.65.Ud

Keywords: Entanglement entropy; Color confinement; Large N gauge theory; Gauge/string duality; Phase transition

* Corresponding author.
E-mail address: arvind@princeton.edu (A. Murugan).

0550-3213/$ – see front matter © 2008 Elsevier B.V. All rights reserved.
doi:10.1016/j.nuclphysb.2007.12.017

1. Introduction

Consider a $(d+1)$-dimensional quantum field theory (QFT) on $\mathbb{R}^{d+1}$ in its vacuum state $|0\rangle$. Divide the d-dimensional space into two complementary regions,

$$A = \mathbb{R}^{d-1} \times I_l,$$
$$B = \mathbb{R}^{d-1} \times (\mathbb{R} - I_l), \tag{1}$$

where I_l is a line segment of length l. The entanglement entropy between the regions A and B is defined as the entropy seen by an observer in A who does not have access to the degrees of freedom in B, or vice versa (see e.g. [1] for a recent review and references to earlier work). It can be calculated by tracing the density matrix of the vacuum, $\rho_0 = |0\rangle\langle 0|$, over the degrees of freedom in B and forming the reduced density matrix

$$\rho_A = \mathrm{Tr}_B\, \rho_0. \tag{2}$$

The quantum entanglement entropy S_A is then given by

$$S_A = -\,\mathrm{Tr}_A\, \rho_A \ln \rho_A. \tag{3}$$

The above construction can be generalized in a number of ways. In particular, one can replace the vacuum state $|0\rangle$ by any other pure or mixed state, and choose the submanifold of $\mathbb{R}^d$, A, to be different than (1). In this paper we will restrict to the choices above, which are sufficient for our purposes.

The entanglement entropy (3) is in general UV divergent. To leading order in the UV cut-off a it scales like [2,3]

$$S_A \simeq \frac{V_{d-1}}{a^{d-1}} \tag{4}$$

where V_{d-1} is the volume of $\mathbb{R}^{d-1}$ in (1). Note that (4) is independent of l. This turns out to be a general feature—the entropy is defined up to an l independent (infinite) additive constant. In particular, $\partial_l S_A$ and differences of entropies at different values of l approach a finite limit as $a \to 0$. In $(d+1)$-dimensional CFT with $d > 1$, the finite l-dependent part of the entropy is negative and proportional to V_{d-1}/l^{d-1}, while for $d = 1$ it goes like $\ln l$.

If the QFT in question has a gravity dual [4], it is natural to ask whether the entanglement entropy can be calculated using the bulk description. This problem was addressed in [5]. For the case of $(d+1)$-dimensional large N_c conformal field theories with AdS_{d+2} gravity duals, the authors of [5] proposed a simple geometric method for computing the entanglement entropy and subjected it to various tests. This method is to find the minimal area d-dimensional surface γ in AdS_{d+1} such that the boundary of γ coincides with the boundary of A, which in the case (1) consists of two copies of $\mathbb{R}^{d-1}$ a distance l apart. The quantum entanglement entropy between the regions A and B is proportional to the classical area of this surface,

$$S_A = \frac{1}{4G_N^{(d+2)}} \int_\gamma d^d\sigma \sqrt{G^{(d)}_{\mathrm{ind}}}, \tag{5}$$

where $G_N^{(d+2)}$ is the $(d+2)$-dimensional Newton constant and $G^{(d)}_{\mathrm{ind}}$ is the induced string frame metric on γ. Note that the surface γ is defined at a fixed time and (5) gives the entanglement

entropy at that time. For static states, such as the vacuum, the resulting entropy is time independent.[1] Also, since γ is extended in the transverse $\mathbb{R}^{d-1}$ (1), the entropy (5) is proportional to its volume V_{d-1}. Thus, in this case it is better to consider the entropy per unit transverse volume.

In non-conformal theories, the volume of the $8-d$ compact dimensions and the dilaton are in general not constant. A natural generalization of (5) to the corresponding ten-dimensional geometries is [5,7]

$$S_A = \frac{1}{4G_N^{(10)}} \int d^8\sigma\, e^{-2\phi} \sqrt{G^{(8)}_{\rm ind}}. \tag{6}$$

The entropy is obtained by minimizing the action (6) over all surfaces that approach the boundary of A (1) at the boundary of the bulk manifold, and are extended in the remaining spatial directions. Since $G_N^{(10)} = 8\pi^6 \alpha'^4 g_s^2$, this gives an answer of order N_c^2 in the 't Hooft limit $N_c \to \infty$ with $g_s N_c$ held fixed.

It was shown in [5] that for AdS_3 the prescription (5) successfully reproduces the known form of the entanglement entropy in two-dimensional conformal field theory, and that it gives sensible results when applied to some higher-dimensional vacua, such as $AdS_5 \times S^5$. Nevertheless, some aspects of the proposal are not well understood. In particular, it is not clear how to extend it beyond leading order in $1/N_c$.

In this paper we apply the proposal of [5,7] to confining backgrounds, such as [8,9]. One of the motivations for this investigation is to subject the proposal (6) to further tests. Another is to study the l dependence of the entanglement entropy, which is in general difficult to determine in strongly coupled field theories.

Gravitational backgrounds dual to confining gauge theories typically have the following structure. As one moves in the radial direction away from the boundary, an internal cycle smoothly contracts and approaches zero size at the infrared (IR) end of space. The radial direction together with the shrinking cycle make a type of cigar geometry, with the IR end of space corresponding to the tip of the cigar.

We will see that in such geometries there are in general multiple local minima of the action (6) for given l. One of those is a disconnected surface, which consists of two cigars extended in $\mathbb{R}^{d-1}$ and separated in the remaining direction in $\mathbb{R}^d$ by the distance l. A second one is a connected surface, in which the two cigars are connected by a tube whose width depends on l. Since the two geometries are related by a continuous deformation, there is a third extremum of the action between them, which is a saddle point of (6). A natural generalization of the proposal of [5] to this case is to identify the entanglement entropy with the absolute minimum of the action. We will see that this leads to a phase transition in the behavior of the entanglement entropy as a function of l.[2]

For the disconnected solution, S_A (6) does not depend on l. As mentioned above, the actual value of S_A depends on the UV cut-off, but if we are only interested in differences of entropies, or the derivative of the entropy with respect to l, we can set it to zero. For the connected solution, S_A depends non-trivially on l. For small l, it is smaller than that of the disconnected one. Thus, it dominates the entropy (6). For $l > l_{\rm crit}$ the action of the connected solution becomes larger than that of the disconnected one, and it is the latter that governs the entropy. Thus, in going from

[1] Generalizations of the proposal of [5] to time-dependent states were discussed in [6].

[2] This phenomenon has already been noted in one specific example [7]—the static "AdS bubble", which is equivalent to the background of D3-branes on a circle that we study in Section 4 (we thank T. Takayanagi for pointing this out to us).

$l < l_{\rm crit}$ to $l > l_{\rm crit}$, $\partial_l S_A$ goes from being of order N_c^2 to being of order N_c^0. One can think of this change of behavior as a phase transition which, as we show, is typical in large N_c confining theories.

Similar transitions between connected and disconnected D-brane configurations play a role in other contexts. In [10] an analogous transition is responsible for screening of magnetic charges in confining gravitational backgrounds; in [11] it governs the pattern of metastable supersymmetry breaking vacua in a brane construction of supersymmetric QCD. An important difference is that in all these cases the transitions involve the rearrangement of real branes, whereas the hypersurface whose area is being minimized here does not seem to have such an interpretation.

The plan of the rest of the paper is as follows. In Section 2 we present a general analysis of a class of gravitational backgrounds that arises in the construction of holographic duals of confining gauge theories. We show that in this class there are multiple local minima of the action (6), as discussed above. With some mild assumptions, we also show that for small l the global minimum of the action corresponds to a connected solution, while for large l it corresponds to a disconnected one. We also show that the connected solution does not exist for sufficiently large l.

In Sections 3–5 we illustrate the discussion of Section 2 with a few examples. Section 3 contains an analysis of the geometry of N_c D4-branes wrapped around a circle with twisted boundary conditions for the fermions. For $g_s N_c \ll 1$ this system reduces at low energies to pure Yang–Mills (YM) theory, while for $g_s N_c \gg 1$ it can be analyzed using the near-horizon geometry of the D4-branes [8]. In Section 4 we describe the analogous D3-brane system, which for $g_s N_c \ll 1$ gives rise to YM in $2+1$ dimensions. Some of the results of this section were obtained already in [7]. Section 5 contains an analysis of the warped deformed conifold (KS) background [9], which corresponds to a cascading, confining $SU(M(k+1)) \times SU(Mk)$ supersymmetric gauge theory. This theory approaches pure $SU(M)$ SYM theory in the limit $g_s M \ll 1$, while the dual supergravity description is reliable in the opposite limit, $g_s M \gg 1$.

In Section 6 we connect the results of Sections 2–5 to large N_c confining field theories such as pure YM. To leading order in $1/N_c$, such theories are expected to reduce to free field theories of the gauge singlet bound states. The latter are expected to have a Hagedorn density of states at high mass, $\rho(m) \sim m^\alpha \exp(\beta_H m)$. The entanglement entropy in such theories can be calculated by summing the contributions of the individual states. We show that this sum over states has a very similar character to the finite temperature partition sum, with l playing the role of the inverse temperature β. It converges for sufficiently large l and diverges below a critical value of l, since the large entropy overwhelms the exponential suppression of the contribution of a given state of large mass. In the thermodynamic case, this phenomenon is related to the appearance of a deconfinement transition. By analogy, it is natural to expect that here it signifies a transition between an entropy that goes like N_c^0 at large l, and one that goes like N_c^2 below a critical value. Since the gravitational analysis reproduces this feature of the dynamics, we conclude that the system with $g_s N_c \gg 1$ is in the same universality class as the one with $g_s N_c \ll 1$.

In Section 7 we comment on our results and discuss other systems which one can analyze using similar techniques. We also point out some general issues related to the proposal of [5].

2. Holographic computation of entropy

The gravitational backgrounds we will consider have the string frame metric

$$ds^2 = \alpha(U)\left[\beta(U)\,dU^2 + dx^\mu\,dx_\mu\right] + g_{ij}\,dy^i\,dy^j, \tag{7}$$

where x^μ ($\mu = 0, 1, \ldots, d$) parametrize $\mathbb{R}^{d+1}$, U is the holographic radial coordinate, and y^i ($i = d+2, \ldots, 9$) are the $8-d$ internal directions. The volume of the internal manifold,

$$V_{\rm int} = \int \prod_{i=1}^{8-d} dy^i \sqrt{\det g}, \tag{8}$$

and the dilaton, ϕ, are taken to depend only on U.

The radial coordinate U ranges from a minimal value, U_0, to infinity. As $U \to U_0$, a p-cycle in the internal $(8-d)$-dimensional space shrinks to zero size, so $V_{\rm int}(U_0) = 0$. The vicinity of $U = U_0$ looks locally like the origin of spherical coordinates in $\mathbb{R}^{p+1}$ (times a compact space), and we assume that all the supergravity fields are regular there. In particular, $\alpha(U)$ and $\phi(U)$ approach fixed finite values as $U \to U_0$. The fact that $\alpha(U_0) > 0$ implies that the string tension is non-vanishing. This is the gravitational manifestation of the fact that the dual gauge theory is confining.

Examples of backgrounds in this class that will be discussed below are the geometries of coincident D3- and D4-branes on a circle with twisted boundary conditions [8], in which the shrinking cycle is a circle ($p = 1$), and the KS geometry [9] in which it is a two-sphere ($p = 2$). In the D3-brane and KS cases, the dilaton is independent of U.

We would like to use the proposal (6) to calculate the entanglement entropy of A and B (1) in the geometry (7). Denoting the direction along which the line segment I_l in (1) is oriented by x, the entropy per unit volume in the transverse $\mathbb{R}^{d-1}$ is given by

$$\frac{S_A}{V_{d-1}} = \frac{1}{4G_N^{(10)}} \int_{-l/2}^{l/2} dx \sqrt{H(U)} \sqrt{1 + \beta(U)(\partial_x U)^2} \tag{9}$$

where we introduced the notation

$$H(U) = e^{-4\phi} V_{\rm int}^2 \alpha^d. \tag{10}$$

Due to the shrinking of the p-cycle, we have $H(U_0) = 0$. Thus, as U varies between U_0 and ∞, $H(U)$ varies between 0 and ∞. It provides a natural parametrization of the radial direction of the space (7). Near U_0, one has $H \sim r^{2p}$, where $r \in [0, \infty)$ is a natural radial coordinate, $dr = \sqrt{\beta(U)}\, dU$.

The quantity (10) is simply related to the warp factor we get upon dimensionally reducing on the $(8-d)$-dimensional compact manifold. The resulting $(d+2)$-dimensional Einstein frame metric may be written as

$$ds_{d+2}^2 = \kappa(U)\big[\beta(U)\, dU^2 + dx^\mu\, dx_\mu\big]. \tag{11}$$

A standard calculation shows that $\kappa(U)^d = H(U)$. It is a common assumption that the warp factor $\kappa(U)$ is a monotonic function of the holographic radial coordinate. In particular, finiteness of the holographic central charge [12],

$$c \sim \beta^{d/2} \kappa^{3d/2} (\kappa')^{-d}, \tag{12}$$

requires κ to be monotonic. Since it goes to zero as $U \to U_0$ and to infinity as $U \to \infty$, it must be that $\kappa' > 0$ for all U. This implies $H'(U) > 0$, a fact that will be useful below.

We need to find the shape $U(x)$ that minimizes the action (9) subject to the constraint $U(x \to \pm\frac{l}{2}) \to \infty$. Denoting by U^* the minimal value of U along this curve,[3] and using the fact that the action does not depend directly on x, its equation of motion can be integrated once and written in the form

$$\partial_x U = \pm\frac{1}{\sqrt{\beta}}\sqrt{\frac{H(U)}{H(U^*)} - 1}. \tag{13}$$

Integrating once more we find

$$l(U^*) = 2\sqrt{H(U^*)}\int_{U^*}^{\infty} \frac{dU\,\sqrt{\beta(U)}}{\sqrt{H(U) - H(U^*)}}. \tag{14}$$

Plugging (13) into (9) we find

$$\frac{S_A}{V_{d-1}} = \frac{1}{2G_N^{(10)}}\int_{U^*}^{U_\infty} \frac{dU\,\sqrt{\beta(U)}H(U)}{\sqrt{H(U) - H(U^*)}}. \tag{15}$$

In the examples we study below, and probably much more generally, the integral in (14) turns out to be convergent, while that in (15) is not. This is the reason for the appearance of the UV cut-off U_∞ in the latter and its absence in the former.

As mentioned earlier, the entropy S_A depends on the cut-off only via an l independent constant, which cancels in differences of entropies. This can be seen from (15) as follows. Denoting by U_1^* and U_2^* the solutions of (14) for $l = l_1$ and $l = l_2$, respectively, we have

$$S_A(l_1) - S_A(l_2) \sim \int^{\infty} dU\,\sqrt{\beta(U)H(U)}\left[\left(1 - \frac{H(U_1^*)}{H(U)}\right)^{-1/2} - \left(1 - \frac{H(U_2^*)}{H(U)}\right)^{-1/2}\right] \tag{16}$$

where we omitted an overall multiplicative constant and focused on the behavior of the integral in the UV region $U \to \infty$. In that region $H(U) \to \infty$, and we can approximate the integrand in (16) by

$$S_A(l_1) - S_A(l_2) \sim \left(H(U_1^*) - H(U_2^*)\right)\int^{\infty} dU\sqrt{\frac{\beta(U)}{H(U)}}. \tag{17}$$

The integrand in (17) behaves as $U \to \infty$ in the same way as that in (14). Thus, if the latter is finite and does not require introduction of a UV cut-off, the same is true for the former.

To find the dependence of the entropy on l we need to determine $U^*(l)$ by solving (14), and then use it in (15). In the next sections we will study specific examples of this procedure; here we would like to make some general comments on it.

Consider first the limit $U^* \to \infty$. Physically, one would expect $l(U^*)$ to go to zero in this limit since as $l \to 0$ the minimal action surface should be located at larger and larger U. In terms of (14) this means that although the prefactor $\sqrt{H(U^*)}$ goes to infinity, the integral goes to zero faster, such that the product of the two goes to zero as well. We will see below that this is indeed what happens in all the examples we will consider.

[3] If the curve is smooth, this value is attained at $x = 0$, where $\partial_x U = 0$.

It turns out that l (14) also goes to zero in the opposite limit $U^* \to U_0$. The prefactor $\sqrt{H(U^*)}$ goes to zero in this limit, and as long as the integral does not diverge rapidly enough to overwhelm it, $l \to 0$. Since any divergence of the integral as $U^* \to U_0$ must come from the region $U \simeq U^* \simeq U_0$, it is enough to estimate the contribution to it from this region. In terms of the coordinate r defined above, one has

$$l(r_*) \sim r_*^p \int\limits_{r_*} \frac{dr}{\sqrt{r^{2p} - r_*^{2p}}}. \tag{18}$$

For $p > 1$ one finds that for small r_*, $l(r_*) \sim r_*$; for $p = 1$, $l(r_*) \sim r_* \ln r_*$. In both cases, $l \to 0$ in the limit $r_* \to 0$ (or, equivalently, $U^* \to U_0$).

We see that for small l the equation of motion (13) has two independent solutions, one with large U^* and the other with $U^* \simeq U_0$. The former is a local minimum of the action (15) while the latter is a saddle point. We can interpolate between them with a sequence of curves which differ in the minimal value of U, such that the solution with large U^* is a local minimum along this sequence, while the one with $U^* \simeq U_0$ is a local maximum.

This implies that there must be another local minimum of the effective action, with U^* smaller than that of the saddle point. This solution cannot correspond to a smooth $U(x)$, since then it would be captured by the above analysis. Therefore, it must correspond to a disconnected solution, which formally has $U^* = U_0$, but is better described as two disconnected surfaces that are extended in all spatial directions except for x, and are located at $x = \pm\frac{l}{2}$.

The entropy corresponding to this solution is given by (see (15))

$$\frac{S_A}{V_{d-1}} = \frac{1}{2G_N^{(10)}} \int\limits_{U_0}^{U_\infty} dU \sqrt{\beta(U) H(U)}. \tag{19}$$

By the above analysis it must be smaller than that of the connected solution with $U^* \simeq U_0$, but may be larger or smaller than that of the connected local minimum with large U^*.

We saw before that $l(U^*)$, (14), goes to zero both at large U^* and as $U^* \to U_0$. If the supergravity background is regular, one can show that between these two extremes l is a smooth function of U^*, that remains finite everywhere. The simplest behavior it can have is to increase up to some point where $\partial l/\partial U^* = 0$, and then decline back to zero as $U^* \to \infty$. We will see that this is indeed what happens in all the examples we study below.

Denoting the value of $l(U^*)$ at the maximum by $l_{\max}$, this behavior implies that smooth solutions to the equation of motion (13) only exist for $l \leqslant l_{\max}$. As $l \to l_{\max}$ from below, the local minimum and saddle point discussed above approach each other, merge and annihilate for $l > l_{\max}$.

At first sight, the fact that there are no solutions to (13) for $l > l_{\max}$ may seem puzzling, but it is important to remember that this analysis only captures smooth connected solutions. As discussed above, for all l we have in addition a disconnected solution for which $U'(x)$ is infinite. For $l > l_{\max}$ the entanglement entropy S_A is governed by this solution and is given by (19). For $l < l_{\max}$ one needs to compare the entropies of the connected and disconnected solutions and find the smaller one. This difference can be written as

$$\frac{2G_N^{(10)}}{V_{d-1}}\left(S_A^{(\text{conn})} - S_A^{(\text{disconn})}\right) = \int\limits_{U^*}^{\infty} dU \sqrt{\beta H}\left(\frac{1}{\sqrt{1 - \frac{H(U^*)}{H(U)}}} - 1\right) - \int\limits_{U_0}^{U^*} dU \sqrt{\beta H}. \tag{20}$$

It is physically clear and easy to see from (20) that for small l the connected solution with large U^* has the lower entropy. As l increases, there are in general two possibilities. The connected solution can remain the lower action one until $l = l_{\rm max}$, or there could be a critical value $l_{\rm crit} < l_{\rm max}$ above which the right-hand side of (20) is positive, so that the disconnected solution becomes the dominant one. In the first case there would be a phase transition at $l = l_{\rm max}$; in the second, the transition would occur at $l_{\rm crit}$, and in the range $l_{\rm crit} < l < l_{\rm max}$, the connected solution would be a metastable local minimum. In all the examples we study below it is the second possibility, $l_{\rm crit} < l_{\rm max}$, that is realized: as we increase l, the transition occurs before the connected solution ceases to exist. This is similar to the first-order finite temperature deconfinement transitions found in gravitational duals of confining gauge theories [8,13–15].

3. D4-branes on a circle

The low energy dynamics of N_c D4-branes in type IIA string theory is governed by $(4+1)$-dimensional supersymmetric Yang–Mills theory with gauge group $U(N_c)$ and 't Hooft coupling $\lambda = g_s N_c l_s$. In order to reduce to $3+1$ dimensions and break supersymmetry, we compactify one of the directions along the branes, x^4, on a circle of radius R_4, $x^4 \sim x^4 + 2\pi R_4$, with twisted boundary conditions for the fermions.

The low energy dynamics of this system, which was studied in [8], depends on the dimensionless parameter $\lambda_4 = \lambda/R_4$, and can be investigated using different tools in different regions of parameter space. For $\lambda_4 \ll 1$, it corresponds to pure Yang–Mills theory with gauge group $U(N_c)$ and 't Hooft coupling λ_4 (at the scale R_4). In the opposite limit, $\lambda_4 \gg 1$, one can use a gravitational description in terms of the near-horizon geometry of the branes[4]

$$ds^2 = \left(\frac{U}{R}\right)^{3/2}\left[\left(\frac{R}{U}\right)^3 \frac{dU^2}{f(U)} + dx^\mu\, dx_\mu\right] + R^{3/2}U^{1/2}\, d\Omega_4^2 + \left(\frac{U}{R}\right)^{3/2} f(U)\big(dx^4\big)^2, \tag{21}$$

$$e^{-2\phi} = \left(\frac{R}{U}\right)^{3/2}, \tag{22}$$

where R is related to the five-dimensional 't Hooft coupling via the relation $R^3 = \pi\lambda$, and

$$f(U) = 1 - \left(\frac{U_0}{U}\right)^3, \quad U_0 = \frac{4\pi}{9}\frac{\lambda}{R_4^2}. \tag{23}$$

As $U \to U_0$, the radius of the x^4-circle goes to zero; (U, x^4) form together a cigar geometry of the type described in the previous sections.

Comparing (21), to (7) we identify α, β, $V_{\rm int}$ as,

$$\alpha = \left(\frac{U}{R}\right)^{3/2}, \qquad \beta = \left(\frac{R}{U}\right)^3 \frac{1}{f(U)}, \tag{24}$$

$$V_{\rm int} = \frac{8\pi^2}{3}\big(R^3 U\big) \times 2\pi R_4 \left(\frac{U}{R}\right)^{3/4} \sqrt{f(U)} = \frac{32\pi^3 R^{15/4}}{9U_0^{1/2}} U^{7/4}\sqrt{f(U)}. \tag{25}$$

[4] Here and below we set $\alpha' = 1$.

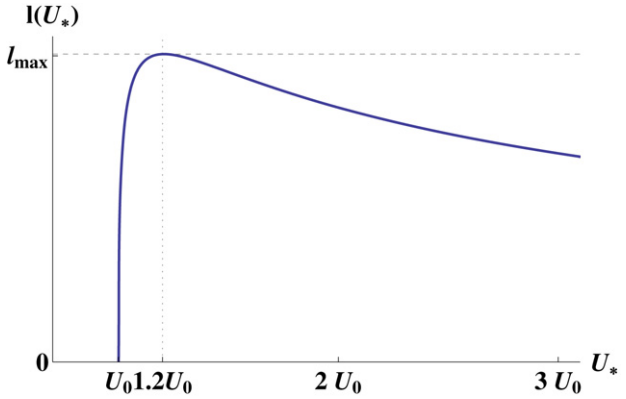

Fig. 1. $l(U^*)$ for D4-branes on a circle.

The combination (10) is given in this case by

$$H(U) = R^6\left(\frac{32\pi^3}{9}\right)^2 \frac{U^2(U^3 - U_0^3)}{U_0}. \tag{26}$$

Note that $H'(U) > 0$ for all $U \geqslant U_0$, as mentioned in the previous section.

The explicit form of the background can be used to verify the assertions of Section 2 about the behavior of $l(U^*)$. In particular, it is easy to check that the integral (14) converges. For $U^* \gg U_0$ it is given by

$$l\big(U^*\big) = 2R^{3/2} \times 2\sqrt{\pi}\,\frac{\Gamma(\frac{3}{5})}{\Gamma(\frac{1}{10})}\,\frac{1}{\sqrt{U^*}}. \tag{27}$$

We see that l indeed goes to zero in the limit $U^* \to \infty$, as expected. Similarly, one can check that it goes to zero in the opposite limit $U^* \to U_0$. The full curve $l(U^*)$ can be computed numerically and is plotted in Fig. 1. It has the qualitative structure anticipated in Section 2. The maximum of the curve occurs at $U^* \simeq 1.2U_0$, with

$$l_{\max} \simeq 1.418 R_4. \tag{28}$$

At larger values of l, there is no smooth solution to the equations of motion (13).

Turning to the entanglement entropy S_A, following the discussion of Section 2 we need to calculate the entropies of the connected solution (15) and the disconnected one (19), and compare them. The calculations of the individual entropies must be done with the UV cut-off U_∞ in place, but the difference of entropies is insensitive to it (see (16), (20)).

For the disconnected solution, the entropy can be calculated in closed form:

$$S_A^{(\text{disconn})} = \frac{8\pi^3}{9}\,\frac{V_2 R^{9/2}}{U_0^{1/2} G_N^{(10)}}\big(U_\infty^2 - U_0^2\big). \tag{29}$$

For the connected one it is given by (15), which in general has to be computed numerically. For small l one can again perform the integral using the fact that in this case $U^* \gg U_0$. One finds

$$S_A^{(\text{conn})}(l) = \frac{8\pi^3}{9}\,\frac{V_2 R^{9/2}}{U_0^{1/2} G_N^{(10)}}\left(U_\infty^2 - 256\left[\frac{\sqrt{\pi}\,\Gamma(\frac{3}{5})}{\Gamma(\frac{1}{10})}\right]^5 \frac{R^6}{l^4}\right). \tag{30}$$

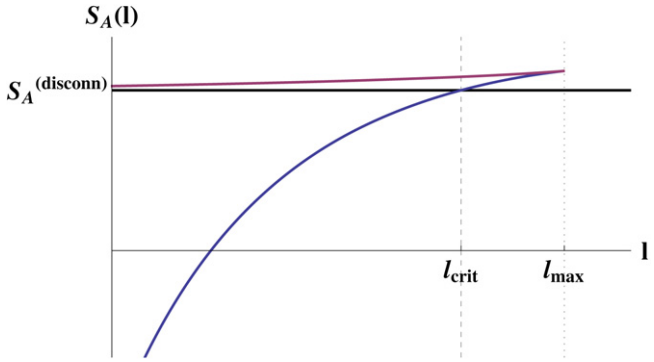

Fig. 2. Entropies of the connected (blue and red) and disconnected (black) solutions for the wrapped D4-brane geometry. (For interpretation of the references to colour in this figure legend, the reader is referred to the web version of this article.)

Comparing to (29) we see that for small l the connected solution has lower entropy, in agreement with the general discussion of Section 2. The fact that the entropy (30) scales like $1/l^4$ at small l is indicative of $(5+1)$-dimensional scale invariant dynamics. This is what one expects, since at short distances the dynamics on the wrapped D4-branes is described by the $(2,0)$ superconformal field theory in $5+1$ dimensions. Indeed, we find

$$S_A^{(\text{conn})}(l) - S_A^{(\text{disconn})} = -V_2(2\pi R_4)(2\pi R_{10})\frac{32\sqrt{\pi}}{3}\left[\frac{\Gamma(\frac{3}{5})}{\Gamma(\frac{1}{10})}\right]^5 \frac{N_c^3}{l^4} + \cdots \tag{31}$$

which is precisely the entanglement entropy of N_c coincident M5-branes compactified on a circle of radius R_4 and the M-theory circle of radius $R_{10} = g_s$ found in [5].

A naive use of (29), (30) suggests that the disconnected solution becomes the lower entropy one at $l \sim R^{3/2}/U_0 \sim R_4$, not far from l_{max} (28). Of course, the small l approximation leading to (30) is not valid there, and in order to determine the precise position of the transition we need to evaluate (15). The result of that evaluation is shown in Fig. 2, where we also exhibit the entropy of the disconnected solution and, for completeness, that of the saddle point discussed in Section 2 as well.

We see that, as expected, the saddle point entropy is larger than that of the connected and disconnected local minima for all l. It approaches that of the connected one as $l \to l_{\text{max}}$, and the disconnected one as $l \to 0$. The entropies of the connected and disconnected solutions cross at $l = l_{\text{crit}} < l_{\text{max}}$ given by

$$l_{\text{crit}} \simeq 1.288 R_4. \tag{32}$$

As explained in Section 2, the entropy is governed by the connected solution and exhibits non-trivial dependence on l for $l < l_{\text{crit}}$, while for $l > l_{\text{crit}}$ it is governed by the disconnected one and is l independent (to leading order in $1/N_c$).

4. D3-branes on a circle

In this section we study the system of N_c D3-branes wrapped around a circle of radius R_3 with twisted boundary conditions for the fermions. The discussion is largely parallel to that of the previous section, and some of the results already appear in [7], so we will be brief.

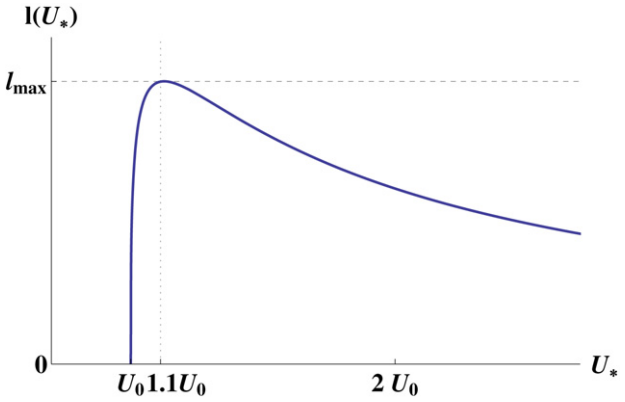

Fig. 3. $l(U_*)$ for D3-branes on a circle.

Before the compactification, the low energy theory on the D3-branes is $N = 4$ SYM with 't Hooft coupling $\lambda = g_s N_c$. For finite R_3 one finds at long distances a $(2+1)$-dimensional confining theory. For $\lambda \ll 1$ that theory is $(2+1)$-dimensional YM with 't Hooft coupling $\lambda_3 = \lambda/R_3$ [8]. For $\lambda \gg 1$ one can instead use a gravitational description in terms of the near-horizon geometry of the N_c D3-branes,

$$ds_{10}^2 = \left(\frac{U}{L}\right)^2 \left[\left(\frac{L}{U}\right)^4 \frac{dU^2}{h(U)} + dx^\mu\, dx_\mu\right] + L^2\, d\Omega_5^2 + \left(\frac{U}{L}\right)^2 h(U)\big(dx^3\big)^2, \tag{33}$$

$$h(U) = 1 - \left(\frac{U_0}{U}\right)^4, \tag{34}$$

where

$$L^4 = 4\pi\lambda, \qquad U_0^2 = \frac{\pi\lambda}{R_3^2}, \tag{35}$$

and the dilaton is constant, $\phi(U) = 0$. Comparing (33) to (7) we find

$$\alpha = \left(\frac{U}{L}\right)^2, \qquad \beta = \left(\frac{L}{U}\right)^4 \frac{1}{h(U)}, \qquad V_{\rm int} = 2\pi^4 R_3 L^4 U \sqrt{h(U)}. \tag{36}$$

The combination (10) is given by

$$H(U) = \big(2\pi^4 R_3\big)^2 L^4 U^6 h(U). \tag{37}$$

It is again monotonically increasing with U, as expected.

All the calculations of the previous section can be done in this case as well. The integral (14) is again convergent. For small l (and large U^*) one finds

$$l\big(U^*\big) = 2\sqrt{\pi}\,\frac{\Gamma(\frac{2}{3})}{\Gamma(\frac{1}{6})}\,\frac{L^2}{U^*}. \tag{38}$$

The extension to all U^* is plotted in Fig. 3. The qualitative shape of $l(U^*)$ is similar to the D4-brane case shown in Fig. 1. The maximum occurs at $U^* \simeq 1.113 U_0$, and

$$l_{\rm max} \simeq 1.383 R_3. \tag{39}$$

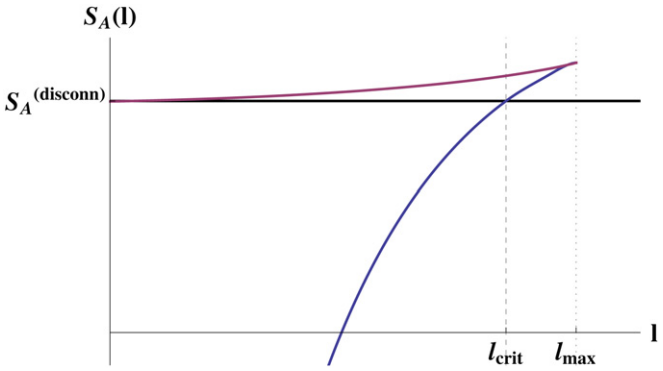

Fig. 4. Entropies of the connected (blue and red) and disconnected (black) solutions for the wrapped D3-brane geometry. (For interpretation of the references to colour in this figure legend, the reader is referred to the web version of this article.)

The entropy of the disconnected solution is given by

$$S_A^{(\text{disconn})} = \frac{\pi^4 R_3 L^4 V_1}{2G_N^{(10)}}\left(U_\infty^2 - U_0^2\right), \tag{40}$$

where V_1 is the length of the strip. The entropy of the connected solution is exhibited in Fig. 4. For small l one has

$$S_A^{(\text{conn})}(l) = \frac{\pi^4 R_3 L^4 V_1}{2G_N^{(10)}}\left(U_\infty^2 - 4\left[\frac{\sqrt{\pi}\,\Gamma(\frac{2}{3})}{\Gamma(\frac{1}{6})}\right]^3 \frac{L^4}{l^2}\right). \tag{41}$$

Therefore, for small l we find

$$S_A^{(\text{conn})}(l) - S_A^{(\text{disconn})} = -2\sqrt{\pi}\left[\frac{\Gamma(\frac{2}{3})}{\Gamma(\frac{1}{6})}\right]^3 V_1 (2\pi R_3)\frac{N_c^2}{l^2} + \cdots \tag{42}$$

which is the entanglement entropy of the $(3+1)$-dimensional $\mathcal{N}=4$ SYM theory compactified on a circle of radius R_3 [5].

As is clear from Fig. 4, the transition between the connected and disconnected solutions happens again at a value of l smaller than l_{max}. The numerical evaluation gives

$$l_{\text{crit}} \simeq 1.2376 R_3. \tag{43}$$

5. Cascading confining gauge theory

The background dual to the cascading $SU(M(k+1)) \times SU(Mk)$ supersymmetric gauge theory is the deformed conifold $\sum_{i=1}^4 z_i^2 = \epsilon^2$ warped by M units of RR 3-form flux. The relevant metric is [9],

$$ds_{10}^2 = h^{-1/2}(\tau)\, dx^\mu\, dx_\mu + h^{1/2}(\tau)\, ds_6^2, \tag{44}$$

where ds_6^2 is the metric of the deformed conifold

$$ds_6^2 = \frac{1}{2}\epsilon^{4/3}K(\tau)\Bigg[\frac{1}{3K^3(\tau)}\big(d\tau^2 + (g^5)^2\big) + \cosh^2\left(\frac{\tau}{2}\right)\big[(g^3)^2 + (g^4)^2\big] + \sinh^2\left(\frac{\tau}{2}\right)\big[(g^1)^2 + (g^2)^2\big]\Bigg]. \tag{45}$$

Here

$$K(\tau) = \frac{\big(\sinh(2\tau) - 2\tau\big)^{1/3}}{2^{1/3}\sinh\tau}, \tag{46}$$

and the warp factor is given by

$$h(\tau) = (g_s M\alpha')^2 2^{2/3}\epsilon^{-8/3}\int_\tau^\infty dx\,\frac{x\coth x - 1}{\sinh^2 x}\big(\sinh(2x) - 2x\big)^{1/3}. \tag{47}$$

The dilaton is constant and we set it to zero. For the details of the angular forms g_i, see [9,16].

The cascading gauge theory has a continuous parameter, $g_s M$. The theory approaches the pure $SU(M)$ SYM theory in the limit $g_s M \to 0$, while the dual supergravity description is reliable in the opposite limit, $g_s M \to \infty$. In this limit the geometry describes a gauge theory with two widely separated scales: the scale of glueball masses,

$$m_{\text{glueball}} = \frac{\epsilon^{2/3}}{g_s M\alpha'}, \tag{48}$$

and the scale of the string tension at the IR end of space (the tip of the cigar), $\sqrt{T_s} \sim \sqrt{g_s M}m_{\text{glueball}}$.

The metric (44), (45) is of the form (7) with

$$\alpha \equiv h^{-1/2}, \qquad \beta \equiv \frac{h(\tau)\epsilon^{4/3}}{6K^2(\tau)}. \tag{49}$$

Using $\int g_1 \wedge g_2 \wedge g_3 \wedge g_4 \wedge g_5 = 64\pi^3$, we get

$$V_{\text{int}} = \frac{4\pi^3}{\sqrt{6}}h^{5/4}\epsilon^{10/3}K\sinh^2(\tau). \tag{50}$$

Thus, all the general formulae of Section 2 apply, with U replaced by the standard deformed conifold radial variable τ.

We find

$$H(\tau) = e^{-4\phi}V_{\text{int}}^2\alpha^3 = \frac{8\pi^6}{3}\epsilon^{20/3}h(\tau)K^2(\tau)\sinh^4(\tau). \tag{51}$$

H can be seen to be monotonically increasing with τ as noted in Section 2 from general considerations. The general equation (14) with these identifications gives $l(\tau_*)$ for the KS background. As in the previous sections, the integral is convergent. For large τ^*, we can approximate $l(\tau)$ using the asymptotic forms valid at large τ,

$$h(\tau) \to 2^{1/3}3(g_s M\alpha')^2\epsilon^{-8/3}\left(\tau - \frac{1}{4}\right)e^{-4\tau/3}, \qquad K \to 2^{1/3}e^{-\tau/3}, \tag{52}$$

$$H(\tau) \to \pi^6\epsilon^4(g_s M\alpha')^2\left(\tau - \frac{1}{4}\right)e^{2\tau}, \qquad \sqrt{\beta} \to 2^{-2/3}\epsilon^{-2/3}(g_s M\alpha')\sqrt{\tau - \frac{1}{4}}e^{-\tau/3}. \tag{53}$$

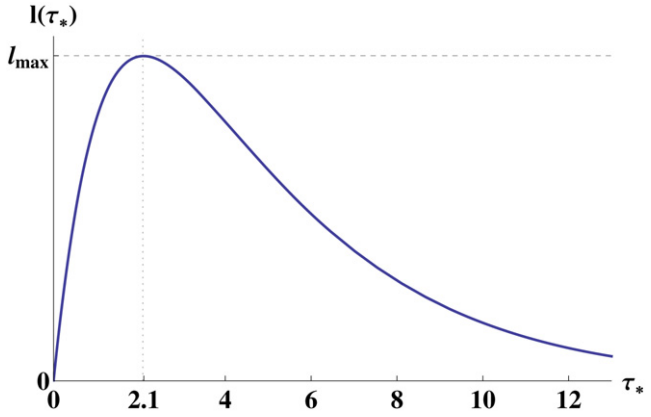

Fig. 5. $l(\tau_*)$ for the KS geometry.

This leads to the simplified expression,

$$l(\tau^*) = 2^{1/3}\epsilon^{-2/3} g_s M\alpha' \int_{\tau^*}^{\infty} \frac{\sqrt{\tau} e^{-\tau/3}\, d\tau}{\sqrt{\frac{\tau e^{2\tau}}{\tau^* e^{2\tau^*}} - 1}}. \tag{54}$$

The main contribution is from the region $\tau \sim \tau^*$; shifting $\tau \to \tau_* + y$ and keeping the lowest order term in y we conclude that for large τ^*,

$$l(\tau^*) = \frac{2^{1/3} 3\sqrt{\pi}\,\Gamma(2/3)}{\Gamma(1/6)} \epsilon^{-2/3} g_s M\alpha' \sqrt{\tau^*} e^{-\tau^*/3}. \tag{55}$$

As earlier, l goes to zero as $\tau^* \to \infty$. One can also verify, as outlined in Section 2, that as $\tau^* \to 0$, l goes to zero again. The full curve, computed numerically, is presented in Fig. 5. We see that it shows the same qualitative behavior as the other cases (Figs. 1, 3). The maximum occurs at $\tau^* \approx 2.1$ with

$$l_{\max} \approx 1.00 m_{\text{glueball}}^{-1}. \tag{56}$$

We now turn to the entanglement entropy S_A. As earlier, we have to calculate and compare the entropies of the connected (15) and disconnected (19) surfaces. As discussed in Section 2, each of these entropies must be computed with a UV cut-off in place, but the difference of the entropies is UV finite. The entropy of the disconnected solution is found to be

$$S_A^{(\text{disconn})} = V_2 \frac{M^2\epsilon^{4/3}}{2^{2/3} 16\pi^3 \alpha'^2} \left(\frac{3}{2}\tau_\infty e^{2\tau_\infty/3} - \frac{21}{8} e^{2\tau_\infty/3} + 2.194 \right) \tag{57}$$

where the finite additive constant was computed numerically. For the connected solution, we first consider an analytic approximation valid for small l:

$$S_A(\tau^*) = V_2 \frac{M^2\epsilon^{4/3}}{2^{2/3} 16\pi^3 \alpha'^2} \int_{\tau^*}^{\tau_\infty} \frac{(\tau - 1/4)^{3/2} e^{5\tau/3}\, d\tau}{\sqrt{(\tau - 1/4)e^{2\tau} - (\tau^* - 1/4)e^{2\tau^*}}}. \tag{58}$$

Approximating this integral as we did for $l(\tau^*)$, we find

$$S_A(\tau^*) = V_2 \frac{M^2\epsilon^{4/3}}{2^{2/3}16\pi^3\alpha'^2} M^2\epsilon^{4/3}\left(\frac{3}{2}\tau_\infty e^{2\tau_\infty/3} - \frac{21}{8}e^{2\tau_\infty/3} - \frac{3\sqrt{\pi}\,\Gamma(2/3)}{2\Gamma(1/6)}\tau^* e^{2\tau^*/3}\right). \tag{59}$$

Thus, for $l \ll 1/m_{\text{glueball}}$,

$$S_A^{(\text{conn})} - S_A^{(\text{disconn})} = -V_2 \frac{243\Gamma(\frac{2}{3})^3}{32\pi^{3/2}\Gamma(\frac{1}{6})^3} \frac{g_s^2 M^4}{l^2} \log^2(m_{\text{glueball}} l) + \cdots. \tag{60}$$

In the cascading theory the effective number of colors is a logarithmic function of the distance scale [9,16,17]:

$$N_{\text{eff}}(l) = \frac{3}{2\pi} g_s M^2 \log(m_{\text{glueball}} l) + \cdots. \tag{61}$$

We see that the finite piece of the entropy is

$$-V_2 \frac{27\sqrt{\pi}\,\Gamma(\frac{2}{3})^3 N_{\text{eff}}^2(l)}{8\Gamma(\frac{1}{6})^3 l^2} + \cdots. \tag{62}$$

For a $(3+1)$-dimensional conformal gauge theory, the finite piece of the entanglement entropy is indeed of the form $N_c^2(V_2/l^2)$. Following [5], we may use a minimal surface in $AdS_5 \times T^{11}$ to find the entanglement entropy in the dual $SU(N) \times SU(N)$ SCFT [18][5]:

$$-V_2 \frac{27\sqrt{\pi}\,\Gamma(\frac{2}{3})^3 N^2}{8\Gamma(\frac{1}{6})^3 l^2}. \tag{63}$$

Hence, the result (62) we find for the cascading gauge theory is a reasonably modified form of the conformal behavior. The same distance-dependent effective number of colors was found in evaluation of correlation functions in the cascading theory [19,20].

Going beyond the small l limit, we present the result of the numerical evaluation of S_A in Fig. 6 which compares the connected, disconnected and saddle point entropies. As expected, the saddle point entropy is always the largest and approaches the disconnected solution for small l and the connected solution as $l \to l_{\max}$. The connected solution has the lowest entropy for small l and is the dominant contribution in this regime. The point at which the connected and disconnected solutions cross is $l_{\text{crit}} < l_{\max}$, which is found to be

$$l_{\text{crit}} \approx 0.95 m_{\text{glueball}}^{-1}. \tag{64}$$

For $l > l_{\text{crit}}$, the $O(N_c^2)$ entropy is l-independent as explained in Section 2.

6. Comparison to field theory

It is natural to ask whether the transition at finite l that we found in confining gravitational backgrounds also occurs in large N_c asymptotically free gauge theories, such as pure YM or $\mathcal{N} = 1$ SYM with gauge group $SU(N_c)$. The location of such a transition would have to be

[5] The extra factor of $27/16$ compared to the result (42) for $AdS_5 \times S^5$ comes from the fact that $\text{vol}(T^{11}) = \frac{16}{27}\,\text{vol}(S^5)$.

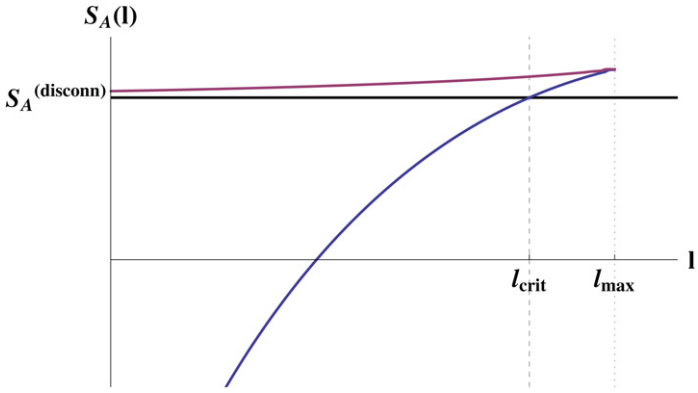

Fig. 6. Entropies of the connected (blue and red) and disconnected (black) solutions for the KS geometry. (For interpretation of the references to colour in this figure legend, the reader is referred to the web version of this article.)

around the QCD scale, $l_{\rm crit}\Lambda_{\rm QCD} \sim 1$. At such scales the theory is strongly coupled and it is difficult to evaluate the entanglement entropy S_A directly.

To proceed one can use the fact that, at large N_c, confining gauge theories are expected to reduce to free field theories of glueballs, whose density of states grows like

$$\rho(m) \simeq m^{\alpha} e^{\beta_H m} \tag{65}$$

at large mass m. The inverse Hagedorn temperature β_H is of order $1/\Lambda_{\rm QCD}$, and α is a constant. Both are difficult to calculate from first principles. Most of the states that contribute to (65) are unstable resonances whose width goes to zero as $N_c \to \infty$. More generally, all interactions between the glueballs go to zero in this limit. At finite N_c the spectrum (65) is effectively cut-off at some large mass scale.

We can use the above picture to calculate the entanglement entropy at large N_c, by summing the contributions of the glueballs. To avoid UV divergences, we will consider the quantity

$$C = l\frac{dS_A(l)}{dl} \tag{66}$$

which, as mentioned in the previous sections, does not depend on the UV cut-off. Consider, for example, a free scalar field of mass m. It is clear that the non-trivial dependence of (66) on l is via the combination ml. We will be interested in the region $ml \gg 1$, where $C(ml)$ can be calculated as follows. In $1+1$ dimensions, the large l form of $C(ml)$ has been obtained in [21]; it is given by

$$C_1(ml) = \frac{ml}{4}K_1(2ml) \simeq \frac{\sqrt{\pi ml}}{8}e^{-2ml}. \tag{67}$$

A four-dimensional free scalar field can be thought of as an infinite collection of two-dimensional ones, labeled by the momentum in the transverse $\mathbb{R}^2$, $\vec{k}$, with mass $m(\vec{k}) = \sqrt{m^2 + \vec{k}^2}$. Summing over these momentum modes we find the $(3+1)$-dimensional version of (67),

$$C_3(ml) = \frac{V_2}{(2\pi)^2}\int d^2\vec{k}\, C_1\big(m(\vec{k})l\big) \simeq \frac{V_2}{32\pi}\frac{\sqrt{\pi}m^2}{\sqrt{ml}}e^{-2ml}. \tag{68}$$

We see that the contribution of a single scalar field to the entanglement entropy is exponentially suppressed at large mass.[6] This is similar to the exponential suppression of its contribution to the canonical partition sum at finite temperature, with the role of the inverse temperature β played here by $2l$.

For a theory with a Hagedorn spectrum (65) of bound states, the total entropy is obtained by summing over all states,

$$C_{\text{total}} = \int dm\, \rho(m) C_3(m) \sim \int^{\infty} dm\, m^{\beta} e^{(\beta_H - 2l)m}. \tag{69}$$

The integral converges for $l > \beta_H/2$ and diverges otherwise. This is the analog of the usual Hagedorn divergence of the canonical partition sum at the Hagedorn temperature. There, the physical picture is that for temperatures below some critical temperature, that is believed to be somewhat below the Hagedorn one [22,23], the system is in the confining phase and the thermal free energy scales like N_c^0. Above that temperature, the system is in a deconfined phase and the free energy scales like N_c^2.

Similarly, for the entanglement entropy in gauge theory we expect that for l above some l_{crit} that is somewhat larger than $\beta_H/2$ the entanglement entropy is of order N_c^0 and is given by the convergent integral (69), while for $l < l_{\text{crit}}$ the entropy is of order N_c^2, in agreement with the divergence of (69).

The resulting picture is qualitatively similar to what we got from the gravity analysis in Sections 2–5. Of course, as usual, the details are expected to differ because in the gravity regime the theory contains two widely separated scales. One is the scale of the lightest glueball masses, which goes like $1/R_4$ in the D4-brane analysis of Section 3, like $1/R_3$ in that of Section 4, and like m_{glueball} (48) in the KS geometry. The other is the scale of massive string excitations living near the tip of the cigar, $\sqrt{T_s}$, which is parametrically higher than the glueball scale. Since the exponential density of states comes from these string modes, we expect β_H to be of order $T_s^{-1/2}$.

The transition point l_{crit} in the gravity regime is instead determined by the inverse of the lightest glueball mass, and is parametrically larger than the Hagedorn scale $T_s^{-1/2}$. Thus, as we decrease l, the transition at $l = l_{\text{crit}}$ to entanglement entropy of order N_c^2 happens long before β_H, $l_{\text{crit}} \gg \beta_H$. For example, in the cascading theory $l_{\text{crit}}/\beta_H \sim \sqrt{g_s M}$.

In the asymptotically free field theory regime, there is a single scale Λ_{QCD} and everything happens around it. One can interpolate between the two regimes by tuning the 't Hooft coupling (e.g. making $g_s M$ small in the KS example). Our results suggest that no phase transition is encountered along such an interpolation—the two regimes are in the same universality class.

The arguments presented above apply directly to large N_c theories. It would be interesting to investigate whether the phase transition we found continues to exist at finite N_c, and to characterize its order. Studying the entanglement entropy in pure glue $SU(N_c)$ lattice gauge theory would therefore be very interesting.

7. Discussion

In this paper we applied the holographic method for calculating the entanglement entropy, introduced in [5], to confining theories with gravity duals. In the simple case of entanglement between a strip of width l and its complement, we found an interesting phase transition as a

[6] The same is true for fermions and other higher spin fields.

function of l: for $l < l_{\rm crit}$ the entropy is dominated by the action of a connected surface, while for $l > l_{\rm crit}$ by that of a disconnected one. After a subtraction of an l-independent UV divergent contribution, we conclude that the entropy is $O(N_c^2)$ for $l < l_{\rm crit}$ and $O(1)$ for $l > l_{\rm crit}$. This transition is qualitatively similar to the confinement/deconfinement transition at finite temperature.

Studying the thermal phase transition in confining gravitational backgrounds requires finding a SUGRA solution with an event horizon, and comparing its action with that of another solution which is horizon-free but has the Euclidean time periodically identified [8]. In general, these calculations are complicated and require a considerable amount of numerical work (see, for example, [13–15]). Studying the qualitatively similar transition for the entanglement entropy is much simpler; instead of finding new SUGRA solutions, one needs to find locally stable surfaces in previously known backgrounds.

We also argued that a transition similar to the one we observed using the methods of [5] should occur in any confining large N_c gauge theory. This reasoning, and the several examples we have presented, make it plausible that any consistent gravity dual of a confining theory has to exhibit this phase transition. This is a useful prediction for any confining gauge/gravity dual pairs that remain to be discovered.

The existence of the transition in the cases we have discussed is linked to p-cycles of the internal geometry that shrink in the IR. One could ask if this is the most general situation that results in the phase transition. As we showed, the monotonic function $H(U) = e^{-4\phi} V_{\rm int}^2 \alpha^d$ has to vanish at the IR "end of space", $U = U_0$. On the other hand, $\alpha(U_0)$ should be non-vanishing for the string to retain its tension in the IR. This seems to restrict us to the vanishing of $e^{-2\phi} V_{\rm int}$. Thus, we should consider models where there are shrinking cycles and/or ϕ diverges in the IR.

Curiously, one of the most widely used gravitational models of confinement [24], AdS_5 with a hard IR wall at $U = U_0$, exhibits neither of these phenomena because both ϕ and $V_{\rm int}$ are assumed to be constant. Therefore, for such a model the transition of the entanglement entropy does not seem to occur. This is not surprising, since the notion of the disconnected solution wrapping the entire geometry is not *a priori* well-defined in this case. A related problem is that the equations of motion are not satisfied at $U = U_0$, hence the boundary conditions are ambiguous there.

There may exist a definition of the boundary conditions that allows the disconnected solution and produces a phase transition of the entanglement entropy (an encouraging sign is that the thermal deconfining transition does take place in the hard-wall model [25]). Indeed, when the hard wall model was considered in [5] the contribution from the part of the minimal surface lying along the hard IR wall was not included in the calculation; hence, it was treated as a disconnected surface. Justifying such a prescription may be a good problem for the future.

Another popular phenomenological model is the "soft wall" model where space–time has the geometry of AdS_5, while $\phi(U)$ blows up in the IR [26]:

$$ds_5^2 = U^2\big(U^{-4}\,dU^2 + dx^\mu\,dx_\mu\big), \qquad \phi(U) = U^{-2}. \tag{70}$$

Here, there is no shrinking internal cycle but the blow-up of the dilaton causes $H(U)$ to rapidly approach zero at $U = 0$.[7] In general, if $H(U) \sim U^p e^{-k/U^q}$ as $U \to 0$, one finds a finite $l_{\rm max}$ (above which the connected solution does not exist) provided $\beta(U)$ has a pole of order $2q + 2$ or less at $U = 0$. One can show this by similar means to those employed in Section 2 where only shrinking cycles were considered. In all the models considered in this paper so far, $q = 0$ and

[7] For the soft-wall model $\alpha(U) = U^2$, hence the string loses its tension at $U = 0$. However, the model is typically treated as a five-dimensional field theory, so it is not clear if the string tension requirement needs to be imposed.

β had a pole of order less than 2. On the other hand, the soft wall model corresponds to $q = 2$ while $\beta(U) = 1/U^4$ and hence still satisfies the criterion for the existence of a finite $l_{\max}$. For the soft-wall model one finds that there is indeed a transition between the disconnected solution stretching from $U = 0$ to $U = \infty$ and the connected one that becomes unstable for $l > l_{\rm crit}$ and stops existing at $l_{\max}$.

We see that the entanglement entropy may be useful as a simple test of holographic models of confinement. More ambitiously, it would be nice to show that, if the confining background satisfies the supergravity equations of motion (neither the hard-wall nor the soft-wall do), then there is a phase transition of the entanglement entropy.

Finally, it is important to understand the underlying reasons for the success of the geometric method of [5]. This prescription is designed to capture only the leading, $O(N_c^2)$, term in the entanglement entropy. While it has a superficial similarity to probe brane calculations, it does not seem to be consistent to think of the bulk surface that appears in the construction as a brane. Indeed a brane with the worldvolume action (6) would have tension proportional to $1/g_s^2$, and would back-react on the geometry at leading order in g_s. In any case, branes with the right properties do not seem to exist (see e.g. [27]). We need to formulate the problem in semiclassical gravity whose solution to leading order in $G_N^{(10)}$ is the minimization problem proposed in [5]. Hopefully, this can pave the way to finding the $O(N_c^0)$ corrections to the entanglement entropy and comparing them with field theory.

Acknowledgements

We are grateful to Marcus Benna, Oleg Lunin, Juan Maldacena, Dmitry Malyshev and Tadashi Takayanagi for useful discussions. I.K. acknowledges the hospitality of the University of Tokyo, Komaba, and the Aspen Center for Physics, where some of his work on this project was carried out. A.M. and D.K. acknowledge the hospitality of TASI, Boulder where some of this work was carried out. The work of I.K. and A.M. was supported in part by the National Science Foundation under Grant No. PHY-0243680. The work of D.K. is supported in part by the Department of Energy under grant DE-FG02-90ER40560, the National Science Foundation under grant 0529954 and the Joint Theory Institute funded by Argonne National Laboratory and the University of Chicago. Any opinions, findings, and conclusions or recommendations expressed in this material are those of the authors and do not necessarily reflect the views of these funding agencies.

References

[1] P. Calabrese, J.L. Cardy, Entanglement entropy and quantum field theory: A non-technical introduction, Int. J. Quantum Inf. 4 (2006) 429, quant-ph/0505193.

[2] L. Bombelli, R.K. Koul, J.H. Lee, R.D. Sorkin, A quantum source of entropy for black holes, Phys. Rev. D 34 (1986) 373.

[3] M. Srednicki, Entropy and area, Phys. Rev. Lett. 71 (1993) 666, hep-th/9303048.

[4] J. Maldacena, The large N limit of superconformal field theories and supergravity, Adv. Theor. Math. Phys. 2 (1998) 231, hep-th/9711200;
S.S. Gubser, I.R. Klebanov, A.M. Polyakov, Gauge theory correlators from noncritical string theory, Phys. Lett. B 428 (1998) 105, hep-th/9802109;
E. Witten, Anti-de Sitter space and holography, Adv. Theor. Math. Phys. 2 (1998) 253, hep-th/9802150.

[5] S. Ryu, T. Takayanagi, Holographic derivation of entanglement entropy from AdS/CFT, Phys. Rev. Lett. 96 (2006) 181602, hep-th/0603001;
S. Ryu, T. Takayanagi, Aspects of holographic entanglement entropy, JHEP 0608 (2006) 045, hep-th/0605073.

[6] V.E. Hubeny, M. Rangamani, T. Takayanagi, A covariant holographic entanglement entropy proposal, JHEP 0707 (2007) 062, arXiv: 0705.0016 [hep-th].
[7] T. Nishioka, T. Takayanagi, AdS bubbles, entropy and closed string tachyons, JHEP 0701 (2007) 090, hep-th/0611035.
[8] E. Witten, Anti-de Sitter space, thermal phase transition, and confinement in gauge theories, Adv. Theor. Math. Phys. 2 (1998) 505, hep-th/9803131.
[9] I.R. Klebanov, M. Strassler, Supergravity and a confining gauge theory: Duality cascades and χSB-resolution of naked singularities, JHEP 0008 (2000) 052, hep-th/0007191.
[10] A. Brandhuber, N. Itzhaki, J. Sonnenschein, S. Yankielowicz, Wilson loops, confinement, and phase transitions in large N gauge theories from supergravity, JHEP 9806 (1998) 001, hep-th/9803263.
[11] A. Giveon, D. Kutasov, Gauge symmetry and supersymmetry breaking from intersecting branes, Nucl. Phys. B 778 (2007) 129, hep-th/0703135.
[12] L. Girardello, M. Petrini, M. Porrati, A. Zaffaroni, Novel local CFT and exact results on perturbations of $N = 4$ super-Yang–Mills from AdS dynamics, JHEP 9812 (1998) 022, hep-th/9810126;
D.Z. Freedman, S.S. Gubser, K. Pilch, N.P. Warner, Renormalization group flows from holography supersymmetry and a c-theorem, Adv. Theor. Math. Phys. 3 (1999) 363, hep-th/9904017.
[13] A. Buchel, C.P. Herzog, I.R. Klebanov, L.A. Pando Zayas, A.A. Tseytlin, Non-extremal gravity duals for fractional D3-branes on the conifold, JHEP 0104 (2001) 033, hep-th/0102105;
S.S. Gubser, C.P. Herzog, I.R. Klebanov, A.A. Tseytlin, Restoration of chiral symmetry: A supergravity perspective, JHEP 0105 (2001) 028, hep-th/0102172.
[14] O. Aharony, A. Buchel, P. Kerner, The black hole in the throat—thermodynamics of strongly coupled cascading gauge theories, arXiv: 0706.1768 [hep-th].
[15] M. Mahato, L.A.P. Zayas, C.A. Terrero-Escalante, Black holes in cascading theories: Confinement/deconfinement transition and other thermal properties, arXiv: 0707.2737 [hep-th].
[16] C.P. Herzog, I.R. Klebanov, P. Ouyang, Remarks on the warped deformed conifold, hep-th/0108101.
[17] I.R. Klebanov, A.A. Tseytlin, Gravity duals of supersymmetric $SU(N) \times SU(N + M)$ gauge theories, Nucl. Phys. B 578 (2000) 123, hep-th/0002159.
[18] I.R. Klebanov, E. Witten, Superconformal field theory on threebranes at a Calabi–Yau singularity, Nucl. Phys. B 536 (1998) 199, hep-th/9807080.
[19] M. Krasnitz, A two point function in a cascading $N = 1$ gauge theory from supergravity, hep-th/0011179.
[20] O. Aharony, A. Buchel, A. Yarom, Short distance properties of cascading gauge theories, JHEP 0611 (2006) 069, hep-th/0608209.
[21] H. Casini, M. Huerta, Entanglement and alpha entropies for a massive scalar field in two dimensions, J. Stat. Mech. 0512 (2005) P012, cond-mat/0511014.
[22] J.J. Atick, E. Witten, The Hagedorn transition and the number of degrees of freedom of string theory, Nucl. Phys. B 310 (1988) 291.
[23] J.L.F. Barbon, E. Rabinovici, Touring the Hagedorn ridge, hep-th/0407236.
[24] J. Polchinski, M.J. Strassler, Hard scattering and gauge/string duality, Phys. Rev. Lett. 88 (2002) 031601, hep-th/0109174.
[25] C.P. Herzog, A holographic prediction of the deconfinement temperature, Phys. Rev. Lett. 98 (2007) 091601, hep-th/0608151.
[26] A. Karch, E. Katz, D.T. Son, M.A. Stephanov, Linear confinement and AdS/QCD, Phys. Rev. D 74 (2006) 015005, hep-ph/0602229.
[27] E. Eyras, Y. Lozano, Nucl. Phys. B 573 (2000) 735, hep-th/9908094;
E. Eyras, Y. Lozano, Brane actions and string dualities, hep-th/9812225.